Molecular Pharmacology Fast Forward. Published on October 29, 2014 as DOI: 10.1124/mol.114.094045
This article has not been copyedited and formatted. The final version may differ from this version.

Chaperoning of the A_1-adenosine receptor by endogenous adenosine – an extension of the retaliatory metabolite concept

Justyna Kusek, Qiong Yang, Martin Witek, Christian W. Gruber,

Christian Nanoff and Michael Freissmuth

Institute of Pharmacology, Center of Physiology and Pharmacology,

Medical University of Vienna, Währinger Str. 13a, A-1090 Vienna, Austria

Molecular Pharmacology Fast Forward. Published on October 29, 2014 as DOI: 10.1124/mol.114.094045
This article has not been copyedited and formatted. The final version may differ from this version.

Running Title page

Running title: Chaperoning of A_1-receptors by endogenous adenosine

Corresponding author: Michael Freissmuth; Institute of Pharmacology,
Center of Physiology and Pharmacology, Medical University of Vienna,
Währinger Str. 13a, A-1090 Vienna, Austria
Ph.: +43-1-40160-31371; Fax: +43-1-40160-31371
Email: michael.freissmuth@meduniwien.ac.at

Number of text pages: 32

Word count: Abstract: 250
Introduction: 672
Discussion: 1217

References: 40

Tables: 0

Figures: 8

Abbreviations:

DMEM, Dulbecco's modified Eagle medium; DPCPX, 8-cyclopentyl-1,3-dipropylxanthine; EHNA, erythro-9-(2-hydroxy-3-nonyl) adenine; EndoH, endoglycosidase H; ENT1 & ENT2, equilibrative nucleoside transporter-1 and -2, respectively; ER, endoplasmic reticulum; GPCR, G protein coupled receptor; NBMPR, S-(4-nitrobenzyl)-6-thioinosine; PBS, phosphate buffered saline; PNGase F, peptide-N-glycosidase F; SLC, solute carrier (numbers and letter indicate family and subfamily, respectively); SF-TAP-tag, strep-tactin II-FLAG tandem affinity purification tag; SR 121463, N-tert-butyl-4-[5'-ethoxy-4-(2-morpholin-4-ylethoxy)-2'-oxospiro[cyclohexane-1,3'-indole]-1'-yl]sulfonyl-3-methoxybenzamide (=satavaptan); XAC, xanthine amine congener

Molecular Pharmacology Fast Forward. Published on October 29, 2014 as DOI: 10.1124/mol.114.094045
This article has not been copyedited and formatted. The final version may differ from this version.

Abstract

Cell-permeable orthosteric ligands can assist folding of G protein coupled receptors in the endoplasmic reticulum (ER); this pharmacochaperoning translates into increased cell surface levels of receptors. Here we used a folding-defective mutant of human A_1-adenosine receptor as a sensor to explore, if endogenously produced adenosine can exert a chaperoning effect. This A_1-receptor-$Y^{288}A$ was retained in the ER of stably transfected HEK293 cells but rapidly reached the plasma membrane in cells incubated with an A_1-antagonist. This was phenocopied by raising intracellular adenosine levels with a combination of inhibitors of adenosine kinase, adenosine deaminase and the equilibrative nucleoside transporter: mature receptors with complex glycosylation accumulated at the cell surface and bound an A_1-selective antagonist with an affinity indistinguishable form the wild type A_1-receptor. The effect of the inhibitor combination was specific, because it did not result in enhanced surface levels of two folding-defective human V_2-vasopressin receptor mutants, which were susceptible to pharmacochaperoning by their cognate antagonist. Raising cellular adenosine levels by subjecting cells to hypoxia (5% O_2) reproduced chaperoning by the inhibitor combination and enhanced surface expression A_1-receptor-$Y^{288}A$ within 1 h. These findings were recapitulated for the wild-type A_1-receptor. Taken together, our observations document that endogenously formed adenosine can chaperone its cognate A_1-receptor. This results in a positive feedback loop that has implications for the retaliatory metabolite concept of adenosine action: if chaperoning by intracellular adenosine results in elevated cell surface levels of A_1-receptors, these cells will be more susceptible to extracellular adenosine and thus more likely to cope with metabolic distress.

Molecular Pharmacology Fast Forward. Published on October 29, 2014 as DOI: 10.1124/mol.114.094045
This article has not been copyedited and formatted. The final version may differ from this version.

Introduction

It is intuitively evident that the density of receptors at the cell surface determines the magnitude of the cellular response to their cognate extracellular ligands. This has been repeatedly verified for G protein coupled receptors (GPCRs). In fact, depending on the mode by which a given receptor engages its cognate G protein(s), there are two possible effects of increasing receptor surface levels: (i) if the receptor has access to all G proteins on the cell surface, the resulting unrestricted collision coupling translates increases in receptor density in shifts of the concentration-response curve to the left. An impressive example is the transgenic overexpression of β_2-adrenergic receptors in the murine heart, which shifts the concentration-response curve for isoproterenol-induced cAMP accumulation by an order of magnitude to the left (Milano et al, 1994). (ii) Alternatively, a receptor undergoes restricted collision coupling. In this instance, an increase in receptor number results in an increased maximum response rather than a shift in the EC_{50} (Keuerleber et al., 2012). The number of receptors is determined by the rate of their delivery to the cell surface and by their removal and recycling. The latter process is understood in considerable detail (Hanyaloglu and von Zastrow, 2008). Receptor expression is obviously regulated by changes in mRNA transcription and stability. In contrast, it is not clear to which extent receptor levels are dependent on the rate of their export from the ER. Like all other integral membrane proteins, GPCRs are synthesized in the ER; their hydrophobic core, which is comprised of the seven transmembrane helices, is inserted via the SEC61 translocon channel into the endoplasmic reticulum. In the nascent polypeptide chain, the transmembrane helices are sequentially released into the lipid bilayer by lateral gating of the SEC61 channel (Park and Rapoport, 2012). Because helices exit individually (or as pairs), annular packing of the helices can only be initiated, after all helices have emerged from the SEC61 channel. Accordingly, folding rather than receptor

Molecular Pharmacology Fast Forward. Published on October 29, 2014 as DOI: 10.1124/mol.114.094045
This article has not been copyedited and formatted. The final version may differ from this version.

synthesis is likely to be rate-limiting (Nanoff and Freissmuth, 2012). Circumstantial evidence supports this conjecture: (i) a considerable fraction of newly synthesized δ-opioid and A_1-adenosine receptors is misfolded and is eliminated by sequential ubiquitination, retrotranslocation and proteasomal degradation (Petäjä-Repo et al., 2000 & 2001; Pankevych et al., 2003). (ii) Conversely, overexpression of a deubiquinating enzyme or inhibition of the proteasome shifts the equilibrium to anterograde trafficking and raises A_{2A}-adenosine receptor surface levels (Milojevic et al., 2006). (iii) Manipulations of the heat-shock protein relay, which assists receptor folding in the ER, affect surface levels of the A_{2A}-adenosine receptor (Bergmayr et al., 2013). (iv) It has long been known that prolonged treatment of β-adrenergic receptors with antagonists can result in exaggerated responses to endogenous agonists, if the treatment is suddenly stopped ("propranolol withdrawal rebound", see Alderman et al., 1974; Miller et al. 1975), because surface receptor levels increase (Aarons et al., 1980). Originally, the increase in receptor expression was attributed to an antagonist-induced inhibition of endocytosis and down-regulation. Currently, this effect is thought to reflect - at least in part - pharmacochaperoning by cell permeable antagonists, *i.e*. orthosteric ligands can assist receptor folding in the ER by binding to and stabilizing conformational intermediates on the trajectory to the stable low energy state of the mature receptor (Morello et al., 2000; Nanoff and Freissmuth, 2012).

Endogenous agonists of GPCRs are not necessarily confined to the extracellular space. Accordingly, they may also accumulate within the cell and thus affect receptor folding. We explored this hypothesis by manipulating cellular levels of adenosine: as a sensor we employed a folding-deficient mutant of the human A_1-adenosine receptor that is exquisitely sensitive to the pharmacochaperoning action of orthosteric ligands, *i.e.* agonists and antagonists (Málaga-Diéguez et al., 2010). Raising endogenous adenosine levels by a combination of enzyme inhibitors that mimics

Molecular Pharmacology Fast Forward. Published on October 29, 2014 as DOI: 10.1124/mol.114.094045
This article has not been copyedited and formatted. The final version may differ from this version.

the effect of hypoxia and by hypoxia did not only promote ER export and cell surface delivery of the mutated but also of the wild type A_1-receptor. Thus, these observations document that a physiological ligand may also act as a chaperone and regulate the level of its target receptor.

Materials and Methods

Materials and receptor constructs

EHNA was purchased from Enzo Life Sciences (Lausen, Switzerland), whereas 5-iodotubercidin, dipyridamole and standard compounds of HPLC grade (adenosine, ATP, ADP, cAMP, AMP) were from Sigma-Aldrich. The sources of other reagents and chemicals are listed in Malaga-Dieguez et al. (2010), which also contains a description of the constructs encoding wild type and mutated versions of the human A_1-adenosine receptor fused to GFP. In addition, we generated N-terminally modified versions thereof by addition of either a FLAG-epitope or a Strep-Tactin II-FLAG tandem affinity purification tag (SF-TAP) at the N-terminus (Gloeckner et al. 2007). Mutant V_2R constructs were a generous gift of Ralf Schülein (Leibniz Institute for Molecular Pharmacology, Berlin). An N-terminal FLAG-tag was added to these receptor constructs by subcloning their cDNA into the Tag-2B expression vector (Stratagene). The integrity of the DNA constructs was verified by fluorescent sequencing.

Cell culture and transfection

Cell cultures were maintained at 37°C in a humidified atmosphere containing 5% CO_2 in DMEM, supplemented with 10% fetal calf serum, 100 units/ml penicillin and 0.1 mg/ml streptomycin. Cells were transfected using the calcium phosphate precipitation method or Turbofect™ (Thermo Scientific). Stable cell lines were generated after transfection by selecting for geneticine (G418) resistance (at a concentration of 0.8 mg/ml) and were screened by radioligand binding. In

Molecular Pharmacology Fast Forward. Published on October 29, 2014 as DOI: 10.1124/mol.114.094045
This article has not been copyedited and formatted. The final version may differ from this version.

hypoxia experiments, cells were incubated in 5% O_2, 5% CO_2 balanced with N_2 for up to 24 hours.

Membrane preparation

Cells were washed twice with PBS, scraped off the plates and centrifuged at 4°C for 10 min at 1,000 g. All following steps were performed on ice or at 4°C. The cell pellets were resuspended in buffer containing 25 mM HEPES.NaOH, pH 7.4, 2 mM $MgCl_2$, 1 mM EDTA and protease inhibitors (Complete™, Roche) and snap-frozen in liquid N_2. After two freeze-thaw cycles, the suspension was forced through a hypodermic needle to disrupt the cell membranes by shearing. The resulting homogenate was diluted 1:5 in buffer and centrifuged at 40,000 g for 20 min. The pellets were resuspended in buffer, frozen in liquid nitrogen and stored at -80°C. Protein concentration was determined colorimetrically by quantifying the formation of Cu^+ with bicinchonic acid (BCA Protein Assay Kit from Thermo Scientific).

Radioligand binding

Cell membranes (10-50 μg of protein/assay) were incubated in a final volume of 0.2 ml buffer containing 25 mM HEPES, pH 7.4, 2 mM $MgCl_2$, 1 mM EDTA buffer, adenosine deaminase (ADA, 1 unit/ml) and the indicated concentrations of [^{3}H]DPCPX (Perkin Elmer; specific activity 110 Ci/mmol). Non-specific binding was determined in the presence of 10 μM XAC (Sigma-Aldrich). The assays were performed in duplicates. After one-hour incubation at room temperature, the reactions were terminated by rapid filtration over glass fibre filters (GF/B, Whatman-GE Healthcare) using a Skatron cell harvester. The filters were dissolved in scintillation medium and counted for radioactivity.

Immunoblotting and enzymatic deglycosylation

Molecular Pharmacology Fast Forward. Published on October 29, 2014 as DOI: 10.1124/mol.114.094045
This article has not been copyedited and formatted. The final version may differ from this version.

Cell membranes (10 – 30 μg of protein) expressing A_1-receptor were loaded onto a SDS-polyacrylamide gel. The resolved proteins were electrophoretically transferred to nitrocellulose membranes, which were blocked with 3% bovine serum albumin in 20 mM Tris.HCl, pH 7.5, 150 mM NaCl, 0.1% Tween 20. Blots were probed with affinity-purified rabbit anti-GFP polyclonal antibodies (1:1500; a gift from Werner Sieghart, Medical University of Vienna) or with antiserum 7 (1:2000) directed against the common N-terminal epitope in G protein β-subunits (Hohenegger et al., 1996) as a loading control. The HRP-conjugated anti-rabbit antibody was used as a secondary antibody (1:5000, GE Healthcare). Immunoreactive bands were visualized by enhanced chemiluminescence (SuperSignal West Pico Chemiluminescent Substrate or SuperSignal West Femto Chemiluminescent Substrate, Thermo Scientific), which was recorded with a CCD camera. The enzymatic deglycosylation was performed on cell membranes using either endo-ß-N-acetylglucosaminidase H (EndoH) or peptide-N-glycosidase F (PNGaseF) according to the protocol provided by the manufacturer (New England Biolabs). The reaction was performed for 16 h at 37°C. The deglycosylated products were visualized by immunoblotting as described above.

Confocal Microscopy

Stably transfected HEK293 cells were seeded onto poly-D-lysine-coated 10-mm glass coverslips. Confocal microscopy was performed as described earlier (Màlaga-Dieguez et al., 2010) using a Zeiss LSM510 confocal microscope (argon laser, 30 mW; helium/neon laser, 1 mW) equipped with an oil immersion objective (Zeiss Plan-Neofluar® 40/1.3). Images were captured with identical microscope settings and analyzed with Fiji (ImageJ) software by applying the same settings for brightness and contrast.

Flow cytometry

Molecular Pharmacology Fast Forward. Published on October 29, 2014 as DOI: 10.1124/mol.114.094045
This article has not been copyedited and formatted. The final version may differ from this version.

HEK293 cells expressing A_1-receptor (approximately 5×10^5) were washed with PBS and detached from the dish bottom with 0.02% EDTA (Sigma). After centrifugation for 5 min at 800 g, cells were resuspended in PBS containing 1% bovine serum albumin. Cells expressing YFP-tagged receptors were washed fixed in 0.3 ml PBS containing 1% paraformaldehyde; for detection of the FLAG-tag, cells were first incubated for 1 h with mouse anti-FLAG M2 primary antibody (1:1000, Stratagene), washed three times in PBS, subsequently incubated in the dark with the Alexa Fluor® 488 goat anti-mouse IgG (1:2000), washed again in PBS and fixed. The suspension was then kept in the dark at 4°C. Cells, which had been incubated only in the presence of the secondary antibody, served as a negative control. Fluorescence of at least 10,000 cells/sample was recorded using a FACSCalibur flow cytometer (BD Biosciences, San Jose, CA) and analyzed with the FlowJo software (BD Biosciences).

Statistics and data analysis

Data are presented as the mean ± SEM. Different conditions were compared using one way analysis of variance (ANOVA) followed by Tukey's post hoc test or by *t*-test with the appropriate Bonferroni correction. Curve fitting was done by non-linear regression using the algorithm provided by GraphPad Prism.

Results

Combined inhibition of adenosine kinase, adenosine deaminase and adenosine transport resulted in accumulation of mature A_1-adenosine receptor-$Y^{288}A$

Point-mutations in the conserved $NP_{xx}Y_{(x)5,6}F$ sequence at the junction of helix seven and the carboxyl terminus/helix eight disrupt surface targeting of the A_1-adenosine receptor and result in

Molecular Pharmacology Fast Forward. Published on October 29, 2014 as DOI: 10.1124/mol.114.094045
This article has not been copyedited and formatted. The final version may differ from this version.

its retention in the ER (Málaga-Diéguez et al., 2010). These mutants can be rescued and their cell surface expression restored upon incubation with cognate ligands, e.g. the antagonist DPCPX. Here, we employed the mutant A_1-receptor-$Y^{288}A$ as a sensor. Our working hypothesis posits that intracellular adenosine can act as an endogenous chaperone for the A_1-adenosine receptor. We explored this conjecture by providing a condition that promotes the accumulation of adenosine within the cell. Adenosine has a short half-life, both within a cell and in the extracellular space and is rapidly redistributed by equilibrative nucleoside transporters ENT1/SLC29A1 and ENT2/SLC29A2 (Olsson and Pearson, 1990). We inhibited the two limbs of adenosine metabolism and prevented its efflux to raise intracellular levels, namely (i) deamination to inosine with the adenosine deaminase inhibitor EHNA, (ii) phosphorylation to AMP with the adenosine kinase inhibitor 5-iodotubercidin, and (iii) efflux via the equilibrative nucleoside transporters by dipyridamole. The combination of these compounds mimics the metabolic changes induced by chronic hypoxia (Kobayashi et al., 2000) and results in elevations of intracellular adenosine (supplementary Fig. 1). Incubation of HEK293 cells stably expressing a YFP-tagged version of A_1-receptor-$Y^{288}A$ in the presence of DPCPX or of the combination of inhibitors (i.e., EHNA, 5-iodotubercidin and dipyridamole) for 24 hours resulted in elevated levels of the receptor protein (*cf*. lanes 1, 2 and 4 in Fig. 1A and Fig. 1B). Blockage of adenosine efflux by dipyridamole or NBMPR (supplementary Fig. 2 A and B) was indispensable for receptor up-regulation, because the effect was not observed in the sole presence of EHNA and 5-iodotubercidin (Fig. 1A, lane 3). This effect was also not present when cells were incubated with only one of the inhibitors (EHNA, dipyridamole or 5-iodotubercidine) (Fig. 1B).

The A_1-receptor immunoreactivity in Fig. 1A migrated as a collection of diffuse bands in the range of 60-72 kDa. This heterogeneity was to be expected because the protein is subject to

Molecular Pharmacology Fast Forward. Published on October 29, 2014 as DOI: 10.1124/mol.114.094045
This article has not been copyedited and formatted. The final version may differ from this version.

sequential glycosylation with modifications of the branched sugar moieties that are stochastic in nature. We incubated the cell membranes carrying wild type (YFP-tagged) A_1-receptor and A_1-receptor-$Y^{288}A$ with the endoglycosidases EndoH and PNGaseF to verify the extent of glycosylation (Fig. 1B). Membrane proteins that reside in the ER carry glycan moieties, which are cleaved by EndoH. In contrast, PNGaseF removes all glycan moieties including the complex, mature glycosylation, which is acquired in the Golgi apparatus. Addition of EndoH resulted in the shift of the band labeled "C" in Fig. 1B to a lower position labeled "D". The upper band (denoted as "M") shifted to the "D" position only upon incubation with *PNGaseF*. Therefore, we concluded that band "C" represents the immature, core-glycosylated receptor species, which resides in the ER. The upper band "M" corresponds to the fully glycosylated, mature form of the receptor. This band accumulated upon treatment with DPCPX and the combination of inhibitors (*cf.* Fig. 1B). The chaperoning effect of DPCPX and the combination of inhibitors (lanes labeled EHNA/IODO/DIP) increased with time and the maximum effect appeared after 24 hours (Fig. 2A). We also visualized the distribution of the receptor within the cells by imaging the YFP-moiety attached to the receptor (supplementary Fig. 3): it is evident that, under basal conditions, the bulk of the mutant A_1-receptor-$Y^{288}A$ resided within the cell and delineated the perinuclear membrane (supplementary Fig. 3A), which is consistent with ER retention. Upon treatment with 1 μM DPCPX (supplementary Fig. 3B) or the combination of inhibitors (supplementary Fig. 3C), the fluorescence was visualized on the cell surface. Note that these images were captured at the same settings as that taken under basal conditions. Because receptor levels increased in the presence of DPCPX and the combination of inhibitors, the images are overexposed.

Molecular Pharmacology Fast Forward. Published on October 29, 2014 as DOI: 10.1124/mol.114.094045
This article has not been copyedited and formatted. The final version may differ from this version.

In most experiments, we observed that DPCPX and the combination of inhibitors increased both, the mature glycosylated and the core glycosylated form of the receptor (*cf.* Fig. 1A). This is consistent with the conjecture that pharmacochaperoning must initially increase the level of receptors in the ER, which are then subsequently exported, by preventing their degradation. We verified this assumption by incubating cells with kifunensine, which inhibits mannosidases required for ERAD (=ER-associated degradation). This resulted in the substantial accumulation of core-glycosylated mutant A_1-receptor-$Y^{288}A$ (Fig. 2B, 3rd lane). However, these additional receptors, which accumulated in the presence of kifunensine, failed to bind the antagonist radioligand [^{3}H]DPCPX (Fig. 2C). In contrast, the receptors, which accumulated in the presence of DPCPX (Fig. 2B, 2nd lane) or the combination of DPCPX and kifunensine (Fig. 2B, 4th lane) did bind the radioligand. This is consistent with the conclusion that a large fraction of the mutant A_1-receptor-$Y^{288}A$ is rapidly degraded, because it is misfolded and thus incapable of binding. In addition, receptor synthesis was blocked by cycloheximide in cells expressing mutant A_1-receptor-$Y^{288}A$ after they had been treated in the absence and presence of DPCPX or the combination of inhibitors (EHNA, dipyridamole and iodotubercidine) for 4 hours. Under these conditions, it was possible to examine the subsequent fate of the mutant A_1-receptor-$Y^{288}A$, which had accumulated in the ER in the absence of any further protein synthesis: Over the next 4 hours, the ER-resident core glycosylated receptor rapidly declined under control condition (*cf.* 55 kDa band in lanes 1, 4 and 7 of Fig. 2D), but the mature glycosylated band did not increase to any appreciable extent (*cf.* bands in the 70 kDa range in lanes 1, 4 and 7 of Fig. 2D). A rapid decrease of the ER-resident receptor was also evident in cells treated in the presence of DPCPX (*cf.* 55 kDa band in lanes 2, 5 and 8 of Fig. 2D), or of the combination of inhibitors (*cf.* 55 kDa band in lanes 3, 6 and 9 of Fig. 2D), but it was accomapied by a concomitant increase in the

Molecular Pharmacology Fast Forward. Published on October 29, 2014 as DOI: 10.1124/mol.114.094045
This article has not been copyedited and formatted. The final version may differ from this version.

mature glycosylated forms of the receptor increased. These observations are also consistent with the conclusion that the ER-resident receptor is degraded unless it is rescued by pharmacochaperoning.

Combined inhibition of adenosine kinase, adenosine deaminase and adenosine transport increased the level of binding-competent mutant A_1-receptor-$Y^{288}A$

We verified that the accumulation of the highly glycosylated species of the A_1-receptor-$Y^{288}A$ translated into higher binding of the antagonist [^{3}H]DPCPX. Binding assays were done with membrane preparations from cells stably expressing two differently tagged versions of the receptor, *i.e.*, with a C-terminal YFP (Fig. 3A) and an SF-TAP tag on the N-terminus (Fig. 3B) at substantially different levels. It is evident from a comparison of Fig. 3A and 3B that the pretreatment with the inhibitors resulted in a comparable relative increase in receptor levels (by about 2.5-fold). We therefore conclude that the nature of the tag did not interfere with the chaperoning action. We also verified separately that neither EHNA, nor 5-iodotubercidin nor dipyridamole *per se*, nor their combination used in the experiments bound to the A_1-receptor in the nanomolar to micromolar range (supplementary Fig. 4). Finally, we also carried out saturation experiments to confirm that the chaperoned receptor recognized the radioligand with high affinity (shown for receptors carrying the N-terminal SF-TAP tag in Fig. 3C; K_D = 4.3±1.6 nM, B_{max} = 486.3±80.0 fmol/mg; K_D = 2.6±0.3 nM, B_{max} = 835.2±34.0 fmol/mg and K_D = 1.0±0.2 nM, B_{max} = 1046.0±42.0 fmol/mg for untreated, DPCPX and inhibitors cocktail conditions, respectively).

Molecular Pharmacology Fast Forward. Published on October 29, 2014 as DOI: 10.1124/mol.114.094045
This article has not been copyedited and formatted. The final version may differ from this version.

Raising intracellular adenosine did not result in the protein accumulation of the V_2-vasopressin receptor folding mutants

A trivial explanation for these observations findings is to assume that a change in adenosine recycling affects cellular ATP levels and thus alters the activity of heat-shock proteins. Accordingly, we compared the ability of the combination of inhibitors to rescue the mutant A_1-receptor-$Y^{288}A$ and mutated versions of the V_2-vasopressin receptor. There are numerous variants of the V_2-receptor, which cause nephrogenic diabetes insipidus because they are retained in the ER due to a folding defect. Their cell surface expression can be restored by pharmacochaperoning with cell permeable antagonists (Wüller et al., 2004). We selected V_2-receptor-$I^{318}S$ and V_2-receptor-$T^{273}R$, which either carried an N-terminal FLAG-tag (Fig. 4B) or a GFP-moiety at the C-terminus (Fig. 4C), and determined their expression level by flow cytometry. The levels of both receptors increased in response to incubation of the cells with the specific antagonist SR121463 for 24 h (left hand panels in Fig. 4B & 4C). However, the combination of inhibitors (EHNA, 5-iodotubercidin and dipyridamole) did not cause any appreciable change in V_2-receptor-$I^{318}S$ and V_2-receptor-$T^{273}R$ (*cf.* bar diagrams in Fig. 4B & 4C, respectively). In contrast, the positive control experiment, which was done in parallel in cells expressing the YFP-tagged A_1-receptor-$Y^{288}A$, showed that both, DPCPX and the combination of inhibitors caused a substantial accumulation of YFP fluorescence (Fig. 4A).

Concentration-dependent effect of 5-iodotubercidin, EHNA and dipyridamole on the accumulation of A_1-adenosine receptor-$Y^{288}A$

As documented above (see Fig. 1A), the three inhibitors must be added in combination to chaperone the A_1-receptor-$Y^{288}A$. We explored which reaction was rate-limiting by incubating

Molecular Pharmacology Fast Forward. Published on October 29, 2014 as DOI: 10.1124/mol.114.094045
This article has not been copyedited and formatted. The final version may differ from this version.

cells expressing the A_1-receptor-$Y^{288}A$ receptor for 24 hours with increasing concentrations of one compound while keeping the other two components constant. The increase in receptor accumulation was determined by flow cytometry and immunoblotting (Fig. 5A and 6A-C). EHNA, 5-iodotubercidin and dipyridamole increased the total levels of the receptor in a concentration-dependent manner with EC_{50}-values in the range of 636± 205, 36± 14 nM and 96± 36 nM, respectively (Fig. 5B). The low EC_{50} of iodotubercidin was also verified by quantifying its effect on receptor accumulation by immunoblotting (Fig. 6A) and by quantifying its effect by radioligand binding, which also gave an EC_{50} of 32± 3 nM (Fig. 6D). EHNA and 5-iodotubercidin inhibit adenosine deaminase with a K_i of 33 nM (Ingolia et al., 1985) and 25 nM (Davies et al., 1984), respectively. The affinity of dipyridamole for human ENT1 and ENT2 is in the range of 5 nM and 350 nM, respectively (Ward et al., 2000). Thus, the EC_{50} for 5-iodotubercidin-induced increase in receptor accumulation closely matched its affinity for adenosine kinase. In contrast, >90% of adenosine deaminase and of ENT1 must be blocked to result in intracellular accumulation sufficient to chaperone the receptor. As noted, sole addition of a single inhibitor did not cause any appreciable increase in receptor levels (Fig. 5C). Similar results were obtained, if receptor expression was analyzed by radioligand binding (supplementary Fig. 5).

Hypoxia-driven ER export of A_1-receptor-$Y^{288}A$

Hypoxia and/or ischemia results in a dramatic increase in tissue levels of adenosine, both within cells and in the extracellular space (Newby, 1984; Olsson and Pearson, 1990). We therefore examined, whether the hypoxia-induced increase in adenosine translated into enhanced folding and subsequent ER export of the mutant A_1-receptor-$Y^{288}A$. This was the case: Fig. 7A, B shows

Molecular Pharmacology Fast Forward. Published on October 29, 2014 as DOI: 10.1124/mol.114.094045
This article has not been copyedited and formatted. The final version may differ from this version.

that, after 24 h incubation under hypoxic conditions (5% of O_2), the mature, fully glycosylated band (band M) increased at the expense of the core-glycosylated form (band C). Thus, hypoxia recapitulated the action of the combination of inhibitors (*cf.* Figs. 7A and 1A&B). The effect was rapid, as it was already detectable as early as after 1 hour incubation under 5% oxygen (Fig. 7B, C). Whereas the pharmacochaperoning action of DPCPX or the combined inhibitors increased up to 24 h (*cf.* Fig. 2A), the effect of hypoxia did not increase further after 2 hours (supplementary Fig. 6). We confirmed that the enhanced accumulation of mature receptor protein translated into an increase in binding competent receptors (Fig. 7C). In cells expressing endogenous A_1-receptors, chronic hypoxia may result in augmented receptor levels as a result of increased transcription of the cognate gene (Hammond et al., 2004), possibly because the promoter contains several candidate binding sites for HIF (hypoxia-inducible factor) (St. Hilaire et al., 2009). However, we placed the A_1-receptor under the control of the CMV promoter. In fact, a hypoxic challenge of HEK 293, in which stable expression of the V_2-receptor-$T^{273}R$ was also driven from the CMV promoter, did not result in accumulation of protein (supplementary Fig. 7).

Combined inhibition of adenosine kinase, adenosine deaminase and adenosine transport or hypoxia increased the levels of wild type A_1-receptor

Taken together our experiments documented that intracellular accumulation of adenosine (caused by inhibition of the enzymes metabolizing adenosine or by hypoxia) facilitated the folding and maturation of the ER-retained mutant of A_1-receptor-$Y^{288}A$. The wild type receptor is also susceptible to pharmacochaperoning, albeit to a lesser extent than folding deficient mutants (Màlaga-Dieguez et al., 2010). Accordingly, we also explored, if the wild type A_1-receptor (carrying an N-terminal FLAG-tag) was subject to endogenously produced adenosine by incubating stably transfected HEK 293 cells for 24 hours in the presence of the combination of

Molecular Pharmacology Fast Forward. Published on October 29, 2014 as DOI: 10.1124/mol.114.094045
This article has not been copyedited and formatted. The final version may differ from this version.

inhibitors. The receptor was detected by flow cytometry via its N-terminal FLAG tag (Fig. 8A & B) or by binding with the antagonist [^{3}H]DPCPX (Fig. 7C&D) and by immunoblotting (Fig. 8E). Pretreatment with the combined inhibitors resulted in more than two-fold increase in mean fluorescence intensity (49.4±11.1, 114.2±36.8 ; Fig. 8A, B) and roughly three-fold increase in binding competent receptors (Fig. 8C, D). The increase in fluorescence, which was detected by flow cytometry must by definition reflect increased cell surface expression, while binding competent receptors can also reside in the ER. We verified receptor maturation independently by examining the effect of the combination of inhibitors on the glycosylation of the (stably expressed) YFP-tagged wild type A_1-receptor: it is evident that this species increased when compared to the untreated control as did the core glycosylated band (*cf.* lanes 1 and 3, Fig. 8E). We also subjected HEK 293 cells expressing the wild type YFP-tagged A_1-receptor to hypoxia (5 % O_2) or hypoxia and the combination of inhibitors (lane 4 in Fig. 8E). After 24 hours, cells subjected to hypoxia had accumulated increased levels of the mature receptor species (lane 2 in Fig. 8E); this was substantially enhanced by the combination of inhibitors (lane 4 in Fig. 8E). Finally, we verified that hypoxia augmented the levels of binding-competent wild type receptors: the saturation hyperbola showed that receptors in membranes from hypoxic cells bound [^{3}H]DPCPX with an affinity indistinguishable from those in control membranes but the levels increased (B_{max}= 12.2±0.3 pmol/mg, K_D = 2.2±0.2 nM and B_{max}=15.0±0.8 pmole/mg, K_D = 1.9±0.3 nM for normoxic and hypoxic conditions, respectively; Fig. 8F). We determined the effect of hypoxia in cells that stably expressed different N-terminally tagged versions of the wild type A_1-receptor (FLAG or SF-TAP) at different levels by exposing the membranes to a single concentration of [^{3}H]DPCPX (10 nM, i.e. close to saturation). On average, hypoxia increased the

Molecular Pharmacology Fast Forward. Published on October 29, 2014 as DOI: 10.1124/mol.114.094045
This article has not been copyedited and formatted. The final version may differ from this version.

levels of receptors by ~20 % regardless of the nature of the tag and of the expression levels; the pooled data are shown in Fig. 8G.

Discussion

It is generally accepted that folding of both, soluble and membrane proteins, is assisted by proteinaceous chaperones. In addition, a large collection of low molecular weight ligands (*e.g.*, metal ions, substrates and cosubstrates, prosthetic groups such as heme etc.) stabilize their target proteins against thermal denaturation: occupancy of their cognate binding site allows these ligands to promote a conformational state that approaches the minimum energy conformation. Accordingly, it is not surprising that these small ligands also chaperone their target proteins during the conformational search associated with folding, regardless of whether they bind to allosteric or orthosteric sites (Leidenheimer and Ryder, 2014). This concept posits that endogenous agonists ought to chaperone their cognate receptors. In the present work, we verified this postulate for the A_1-adenosine receptor by demonstrating that intracellular accumulation of adenosine caused up-regulation of the A_1-adenosine receptor at the cell surface. The increased level of adenosine in the cell was achieved by concerted inhibition of adenosine deaminase, adenosine kinase and equilibrative nucleoside transporters or by application of hypoxia. Adenosine facilitated maturation and ER export of both, (i) a ER-retained receptor with a mutation in the conserved $NP_{xx}Y_{(x)5,6}F$ motif (at the junction of helix 7 and C-tail) and (ii) the wild type receptor. The conclusion that adenosine acted as a chaperone was confirmed by the following evidence. (i) Inhibition of adenosine kinase, deaminase and transport phenocopied the effect of the pharmacochaperone DPCPX and resulted in the accumulation of the mature highly-glycosylated form of the receptor mutant. (ii) Flow cytometry and confocal microscopy provided

Molecular Pharmacology Fast Forward. Published on October 29, 2014 as DOI: 10.1124/mol.114.094045
This article has not been copyedited and formatted. The final version may differ from this version.

an independent confirmation that this treatment up-regulated the A_1-receptor at the cell surface. (iii) Binding experiments confirmed that these additional A_1-receptors were correctly folded, because they bound the antagonist radioligand with an affinity comparable to the wild type receptor. (iv) The effect of adenosine was specific for A_1-adenosine receptor as it did not increase expression of another representative GPCR, namely folding-deficient versions of the V_2-vasopressin receptor. (v) The effect of inhibitors was recapitulated by hypoxia, which is the physiological stimulus to raise adenosine levels.

This chaperoning action of an endogenous ligand on its cognate transmembrane receptor is not unprecedented: at high concentrations (*i.e.*, 1 mM), choline facilitated the ER export and the maturation of heterologously expressed $\alpha_4\beta_2$ nicotinic acetylcholine receptor (Sallette et al., 2005). This observation was recapitulated with another ligand-gated ion channel, namely $GABA_A$-receptors composed of $\alpha_1\beta_2\gamma_{2L}$ pentamers; the chaperoning action was enhanced by co-expression of the GABA-transporter-1/SLC6A1 (Eshaq et al., 2010). Similarly, dopamine chaperones the D_4-receptor and the folding-deficient mutant D_4-receptor-M^{345}T provided that its intracellular concentration is raised by co-expression of the dopamine transporter/SLC6A3 (van Craenenboeck et al., 2005). However, it is difficult to envisage a situation, where the intracellular concentration of choline, GABA or dopamine, reach levels *in vivo* that are compatible with their chaperoning action. The plasma membrane transporters for GABA and dopamine, for instance, operate in a relay with the vesicular transporter, which results in rapid sequestration of neurotransmitters into synaptic vesicles. In contrast, our approach also relied on a physiological manipulation, namely hypoxia. Thus, to the best of our knowledge, the A_1-adenosine receptor is

Molecular Pharmacology Fast Forward. Published on October 29, 2014 as DOI: 10.1124/mol.114.094045
This article has not been copyedited and formatted. The final version may differ from this version.

the first GPCR documented to respond to chaperoning by its endogenous agonist in a physiologically relevant context.

We suspect that our observations are relevant to those receptors, which respond to cell permeable agonists - e.g., the G protein-coupled estrogen receptor GPR30 (Filardo and Thomas, 2012) or endogenous metabolites, which reach high (µM to mM) levels: fatty acids, lactate, ketone bodies, succinate, bile acids activate (recently deorphanized) GPCRs GPR40 and GPR120, the hydrocarboxylic acid receptors (GPR81, GPR109a and GPR109b), GPR91 and TGR5, respectively. These receptors sense the levels of substrates or intermediates of energy metabolism and thus orchestrate the adaptation of the organism to changes in caloric input and demand (Tonack et al., 2012). The ER has been proposed to serve as a reservoir of folding competent GPCR intermediates (Leidenheimer and Ryder, 2014). It is conceivable that, upon an increase of endogenous ligand within the cell, this pool of protein is exported from the ER and traffics to the cell surface. This results in a positive feedback loop that shifts the sensitivity of the target cell. Thus, the adenosine-induced chaperoning of the A_1- receptor is consistent with its role as a retaliatory metabolite (Newby, 1984): the extracellular concentration of adenosine increases after tissue damage and due to hypoxia (Fredholm 2007). *In vivo*, metabolic distress also results in an up to 20-fold increase in intracellular adenosine; in fact, adenosine kinase is particularly sensitive to hypoxia (Decking et al., 1997). Signaling via inhibitory A_1-adenosine receptors suppresses cellular activity (e.g., in the brain or in the heart) and thus counteracts the impact of hypoxia. Based on our observations, we propose that the retaliatory metabolite concept be extended to include adenosine-induced chaperoning of A_1-receptors. This action may not be restricted to A_1-receptors. In fact, in PC12 cells, intracellular A_{2A}-receptors were found to be translocated to the

Molecular Pharmacology Fast Forward. Published on October 29, 2014 as DOI: 10.1124/mol.114.094045
This article has not been copyedited and formatted. The final version may differ from this version.

plasma membranes in response to oxygen deprivation (Arslan et al., 2002). It is attractive to speculate that this increase of A_{2A}-receptors at the cell surface was the result of chaperoning by endogenously formed adenosine.

In class A (rhodopsin-like) GPCRs, the ligand binding pocket is buried in the hydrophobic core, but they engage their (orthosteric) ligands via an entry pathway that is accessible from the extracellular face of the membrane. In the ER, the topological equivalent is the luminal side. It is therefore not clear, how hydrophilic ligands such as dopamine (van Craeneboeck et al., 2005) or adenosine gain access to the receptor to exert their chaperoning action. One possible explanation is the presence of transporters in the ER membranes. In fact, the equilibrative nucleoside transporter-3 (ENT3/SCL29A3) is confined to intracellular membranes and is insensitive to dipyridamole and NBMPR (Baldwin et al., 2005); accordingly it may also be operative in the ER under our experimental conditions. However, an alternative explanation appears more plausible based on the following arguments: molecular dynamics simulations of rhodopsin (Grossfield et al., 2008) and of the β_2-adrenergic receptors (Romo et al., 2010) reveal that activation of the receptors is associated with increased hydration of the ligand binding cavity; in these simulation, the water molecules enter into the hydrophobic core via a pathway that is contiguous with the cytosolic face and eventually adopts the dimension of a water filled channel (Leioatts et al., 2014). In fact, for rhodopsin, it is clear that bulk water rather than the structural water is involved in hydrolytic cleavage of the chromophore (Jastrzebska et al., 2011). Ordered water molecules can also be visualized in the structure of the A_{2A}-adenosine receptor, they extend from the ligand binding pocket to the intracellular face (Liu et al., 2012). Thus, it appears safe to conclude that a hydrophilic pathway exists in many – if not all – rhodospin-like GPCRs. During folding of a

Molecular Pharmacology Fast Forward. Published on October 29, 2014 as DOI: 10.1124/mol.114.094045
This article has not been copyedited and formatted. The final version may differ from this version.

rhodopsin-like GPCR conformational states are likely to be visited, in which this water filled pathway is large enough to allow for entry of orthosteric ligands from the cytosolic side. Possibly, the actions of orthosteric pharmacochaperones is - at least in part - accounted for by their ability to occupy the nascent ligand binding pocket. This ought to both, preclude excessive hydration of the ligand binding cavity and provide additional stabilizing bonds that restrict the mobility of the helices. Thereby folding trajectories are favored that lead to a stable structure.

Molecular Pharmacology Fast Forward. Published on October 29, 2014 as DOI: 10.1124/mol.114.094045
This article has not been copyedited and formatted. The final version may differ from this version.

Acknowledgments. We thank Ralf Schülein (FMP, Forschungsinstitut für Molekulare Pharmakologie, Berlin) and Werner Sieghart (Hirnforschungszentrum/Brain Research Institute, Medical University of Vienna) for generously providing of V_2-receptor encoding plasmids and anti-GFP antibodies, respectively. We gratefully acknowledge the generation of tagged V_2-receptor constructs by Edin Ibrisimovic.

Authorship Contributions.

Participated in research design: Kusek, Nanoff, Freissmuth.

Conducted experiments: Kusek, Yang.

Contributed new reagents or analytic tools: Gruber.

Performed data analysis: Kusek, Nanoff, Freissmuth

Wrote or contributed to the writing of the manuscript: Kusek, Gruber, Nanoff, Freissmuth

Molecular Pharmacology Fast Forward. Published on October 29, 2014 as DOI: 10.1124/mol.114.094045
This article has not been copyedited and formatted. The final version may differ from this version.

References

Aarons RD, Nies AS, Gal J, Hegstrand LR, Molinoff PB (1980) Elevation of β-adrenergic receptor density in human lymphocytes after propranolol administration. *J Clin Invest* **65**:949-957.

Alderman EL, Coltart DJ, Wettach GE, Harrison DC (1974) Coronary artery syndromes after sudden propranolol withdrawal. *Ann Intern Med* **81**:625-627

Arslan G, Kull B, Fredholm BB (2002) Anoxia redistributes adenosine A(2A) receptors in PC12 cells and increases receptor-mediated formation of cAMP. *Naunyn Schmiedebergs Arch Pharmacol* **365**:150-157

Baldwin SA1, Yao SY, Hyde RJ, Ng AM, Foppolo S, Barnes K, Ritzel MW, Cass CE, Young JD (2005) Functional characterization of novel human and mouse equilibrative nucleoside transporters (hENT3 and mENT3) located in intracellular membranes. *J Biol Chem* **280**:15880-15887.

Bergmayr C, Thurner P, Keuerleber S, Kudlacek O, Nanoff C, Freissmuth M, Gruber CW (2013) Recruitment of a cytoplasmic chaperone relay by the A_{2A} adenosine receptor. *J Biol Chem* **288**:28831-28844.

Davies LP, Jamieson DD, Baird-Lambert JA, Kazlauskas R (1984) Halogenated pyrrolopyrimidine analogues of adenosine from marine organisms: pharmacological activities and potent inhibition of adenosine kinase. *Biochem Pharmacol* **33**:347-55.

Decking UKM, Schlieper G, Kroll K, Schrader J (1997) Hypoxia-induced inhibition of adenosine kinase potentiates cardiac adenosine release. *Circ Res* **81**:154–164.

Eshaq RS, Stahl LD, Stone R^{2nd}, Smith SS, Robinson LC, Leidenheimer NJ (2010) GABA acts as a ligand chaperone in the early secretory pathway to promote cell surface expression of $GABA_A$ receptors. *Brain Res* **1346**:1-13.

Filardo EJ, Thomas P (2012) Minireview: G protein-coupled estrogen receptor-1, GPER-1: its mechanism of action and role in female reproductive cancer, renal and vascular physiology. *Endocrinology* **153**:2953-2962.

Fredholm BB (2007) Adenosine, an endogenous distress signal, modulates tissue damage and repair. *Cell Death and Differentiation* **14**:1315–1323.

Gloeckner CJ, Boldt K, Schumacher A, Roepman R, Ueffing M (2007) A novel tandem affinity purification strategy for the efficient isolation and characterisation of native protein complexes. *Proteomics* **7**:4228–4234.

Grossfield A, Pitman MC, Feller SE, Soubias O, Gawrisch K (2008) Internal hydration increases during activation of the G-protein-coupled receptor rhodopsin. *J Mol Biol* **381**(2):478-86.

Hammond LC, Bonnet C, Kemp PJ, Yates MS, Bowmer CJ (2004) Chronic hypoxia up-regulates expression of adenosine A_1 receptors in DDT1-MF2 cells. *Biochem Pharmacol* **67**:421–426

Hanyaloglu AC, von Zastrow M (2008) Regulation of GPCRs by endocytic membrane trafficking and its potential implications. *Annu Rev Pharmacol Toxicol* **48**:537-568.

Hohenegger M, Mitterauer T, Voss T, Nanoff C, Freissmuth M (1996) Thiophosphorylation of the G protein β-subunit in human platelet membranes. Evidence against a direct phosphate transfer reaction to G α-subunits. Mol. Pharmacol. 49: 73–80

Ingolia DE, Yeung CY, Orengo IF, Harrison ML, Frayne EG, Rudolph FB, Kellems RE (1985) Purification and characterization of adenosine deaminase from a genetically enriched mouse cell line. *J Biol Chem* **260**:13261-13267.

Keuerleber S, Thurner P, Gruber CW, Zezula J, Freissmuth M (2012) Reengineering the collision coupling and diffusion mode of the A_{2A}-adenosine receptor: palmitoylation in helix 8 relieves confinement. *J Biol Chem* **287**:42104-42118.

Kobayashi S, Zimmermann H, Millhorn DE (2000) Chronic hypoxia enhances adenosine release in rat PC12 cells by altering adenosine metabolism and membrane transport. *J Neurochem* **74**:621-632.

Jastrzebska B, Palczewski K, Golczak M (2011) Role of bulk water in hydrolysis of the rhodopsin chromophore. *J Biol Chem* **286**:18930-18937.

Leioatts N, Mertz B, Martínez-Mayorga K, Romo TD, Pitman MC, Feller SE, Grossfield A, Brown MF (2014) Retinal ligand mobility explains internal hydration and reconciles active rhodopsin structures. *Biochemistry* 53:376-385.

Leidenheimer NJ, Ryder KG (2014) Pharmacological chaperoning: A primer on mechanism and pharmacology. *Pharmacol Res,* 83:10-19.

Liu W, Chun E, Thompson AA, Chubukov P, Xu F, Katritch V, Han GW, Roth CB, Heitman LH, IJzerman AP, Cherezov V, Stevens RC (2012) Structural basis for allosteric regulation of GPCRs by sodium ions. *Science* 337:232-236.

Málaga-Diéguez L, Yang Q, Bauer J, Pankevych H, Freissmuth M, Nanoff C (2010) Pharmacochaperoning of the A_1 adenosine receptor is contingent on the endoplasmic reticulum. *Mol Pharmacol* **77**:940-952.

Milano CA, Allen LF, Rockman HA, Dolber PC, McMinn TR, Chien KR, Johnson TD, Bond RA, Lefkowitz RJ (1994) Enhanced myocardial function in transgenic mice overexpressing the β_2-adrenergic receptor. *Science* **264**:582-586

Miller RR, Olson HG, Amsterdam EA, Mason DT (1975) Propranolol-withdrawal rebound phenomenon. Exacerbation of coronary events after abrupt cessation of antianginal therapy. *N Engl J Med* **293**:416-418.

Milojevic T1, Reiterer V, Stefan E, Korkhov VM, Dorostkar MM, Ducza E, Ogris E, Boehm S, Freissmuth M, Nanoff C (2006) The ubiquitin-specific protease Usp4 regulates the cell surface level of the A2A receptor. *Mol Pharmacol* **69**:1083-1094.

Morello JP1, Petäjä-Repo UE, Bichet DG, Bouvier M (2000) Pharmacological chaperones: a new twist on receptor folding. *Trends Pharmacol Sci* **21**:466-469.

Nanoff C, Freissmuth M (2012) ER-bound steps in the biosynthesis of G protein-coupled receptors. Subcell Biochem 63:1-21.

Newby AC (1984) Adenosine and the concept of retaliatory metabolites. *Trends Biochem Sci* **9**:42–44.

Olsson RA and Pearson JD (1990) Cardiovascular purinoceptors. *Physiol Rev* **70**:761-845

Park E, Rapoport TA (2012) Mechanisms of Sec61/SecY-mediated protein translocation across membranes. *Annual Rev Biophys* **41**:21–40.

Pankevych H, Korkhov V, Freissmuth M, Nanoff C (2003) Truncation of the A1 adenosine receptor reveals distinct roles of the membrane-proximal carboxyl terminus in receptor folding and G protein coupling. *J Biol Chem* **278**:30283-30293.

Petäjä-Repo UE, Hogue M, Laperriere A, Walker P, Bouvier M (2000) Export from the endoplasmic reticulum represents the limiting step in the maturation and cell surface expression of the human delta opioid receptor. *J Biol Chem* **275**:13727-13736.

Petäjä-Repo UE, Hogue M, Laperriere A, Bhalla S, Walker P, Bouvier M (2001) Newly synthesized human delta opioid receptors retained in the endoplasmic reticulum are

retrotranslocated to the cytosol, deglycosylated, ubiquitinated, and degraded by the proteasome. *J Biol Chem* **276**:4416-4423.

Romo TD, Grossfield A, Pitman MC (2010) Concerted interconversion between ionic lock substates of the β_2-adrenergic receptor revealed by microsecond timescale molecular dynamics. *Biophys J* **98**:76-84.Sallette J, Pons S, Devillers-Thiery A, Soudant M, Prado de Carvalho L, Changeux JP, Corringer PJ (2005) Nicotine upregulates its own receptors through enhanced intracellular maturation. *Neuron* **46**:595-607.

St. Hilaire C, Carroll SH, Chen H, Ravid K (2009) Mechanisms of induction of adenosine receptor genes and its functional significance. *J Cell Physiol* **218**:35-44.

Tonack S, Tang C, Offermanns S (2013) Endogenous metabolites as ligands for G protein-coupled receptors modulating risk factors for metabolic and cardiovascular disease. *Am J Physiol Heart Circ Physiol* **304**:H501-513.

Van Craenenbroeck K1, Clark SD, Cox MJ, Oak JN, Liu F, Van Tol HH (2005) Folding efficiency is rate-limiting in dopamine D4 receptor biogenesis. *J Biol Chem* **280**:19350-19357.

Ward JL, Sherali A, Mo ZP, Tse CM (2000) Kinetic and pharmacological properties of cloned human equilibrative nucleoside transporters, ENT1 and ENT2, stably expressed in nucleoside transporter-deficient PK15 cells. ENT2 exhibits a low affinity for guanosine and cytidine but a high affinity for inosine. *J Biol Chem* **275**:8375-8381.

Wüller S, Wiesner B, Löffler A, Furkert J, Krause G, Hermosilla R, Schaefer M, Schülein R, Rosenthal W, Oksche A (2004) Pharmacochaperones post-translationally enhance cell surface expression by increasing conformational stability of wild-type and mutant vasopressin V2 receptors. *J Biol Chem* **279**:47254-47263

Molecular Pharmacology Fast Forward. Published on October 29, 2014 as DOI: 10.1124/mol.114.094045
This article has not been copyedited and formatted. The final version may differ from this version.

Footnote:

This work was supported by the doctoral program CCHD (Cell Communication in Health and disease), which was jointly funded by grants from the Austrian Science Fund/FWF – Fonds zur Förderung der wissenschaftlichen Forschung [W1205] and the Medical University of Vienna.

Molecular Pharmacology Fast Forward. Published on October 29, 2014 as DOI: 10.1124/mol.114.094045
This article has not been copyedited and formatted. The final version may differ from this version.

Figure Legends

Figure 1. **Accumulation of mature A_1-adenosine receptor-$Y^{288}A$ in cells subjected to an incubation with DPCPX or to inhibition of adenosine kinase, adenosine deaminase and adenosine transport**. A) HEK293 cells stably expressing A_1-receptor-$Y^{288}A$ fused to YFP were incubated for 24 h with vehicle (lane labeled untreated), 1 μM DPCPX as positive control; 2 μM EHNA and 0.5 μM iodotubercidin (IODO) or 2 μM EHNA, 0.5 μM iodotubercidin and 10 μM dipyridamole (EHNA/IODO/DIP). Subsequently, membranes (20 μg/lane) prepared from these cells were electrophoretically resolved and the receptor detected by blotting for the YFP-moiety (upper blot). Immunodetection of G protein β-subunits served as loading control (lower blot). The right hand panel represents the densitometric quantification of the blot, analyzed by ImageJ software. The pixel density of the upper band (~ 70-72 kDa) was determined and normalized by setting the mean density observed in untreated control cells as 1. Data are means from six independent experiments, error bars represent S.E.M. **B) Effect of sole inhibition of adenosine kinase, adenosine deaminase or adenosine transport on the accumulation of mature A_1-adenosine receptor-$Y^{288}A$.** HEK293 cells stably expressing A_1-receptor-$Y^{288}A$ fused to YFP were incubated for 24 h with vehicle (lane labeled untreated), 1 μM DPCPX as positive control and one of the inhibitors: 0.5 μM iodotubercidin (IODO), 2 μM EHNA or 10 μM dipyridamole. Membranes (15 μg/lane) prepared from these cells were separated electrophoretically and immunoblotted as in panel A. The experiment is representative of three independent observations.**C) Comparison of the glycosylation pattern of the wild type A_1-receptor and of the mutant A_1-receptor-$Y^{288}A$ fused to YFP in membranes prepared from cells that had been treated with vehicle (untreated), DPCPX or the combination of inhibitors (IODO/EHA/DIP) as in panel A.** Membranes (10 μg/lane) prepared from cells expressing wild

Molecular Pharmacology Fast Forward. Published on October 29, 2014 as DOI: 10.1124/mol.114.094045
This article has not been copyedited and formatted. The final version may differ from this version.

type and mutant A_1-receptor fused to YFP were incubated overnight with endoglycosidase H or with peptide-N-glycosidase F as outlined under Materials and Methods. The bands are denoted as: M (mature), C (core-glycosylated) and D (de-glycosylated). The experiment was replicated twice more with similar results.

Figure 2. A) Time-dependent accumulation of mutant A_1-receptor-$Y^{288}A$. HEK293 cells stably expressing A_1-receptor-$Y^{288}A$ fused to YFP were incubated for 1, 2, 4, 8, or 24 hours with a vehicle (left hand blot), 1 μM DPCPX (middle blot) or 2 μM EHNA, 0.5 μM iodotubercidin and 10 μM dipyridamole (EHNA/IODO/DIP; right hand blot). Subsequently, membranes (20 μg/lane) prepared form these cells were electrophoretically resolved and the receptor detected by blotting for the YFP-moiety (upper blot). Immunodetection of G protein β-subunits served as loading control (lower blot). A second experiment gave similar results. **B) The folding-defective mutant A_1-receptor-$Y^{288}A$ is eliminated by the ER-associated degradation.** HEK293 cells stably expressing A_1-receptor-$Y^{288}A$ fused to YFP were incubated for 24 hours with a vehicle (lane labeled untreated), 1 μM DPCPX; 2 μM kifunensine (lane labeled KIF) or 1 μM DPCPX and 2 μM kifunensine combined (lane labeled KIF/DPCPX); assay conditions were as outlined in panel A. The right hand panel represents the densitometric quantification of the blot, analyzed by ImageJ software. The pixel density of the immature core-glycosylated (lower) and mature (upper) band were determined and normalized by setting the mean density observed in untreated control cells as 1. Data are means from two independent experiments, error bars represent S.E.M. **C)** HEK293 cells stably expressing A_1-receptor-$Y^{288}A$ fused to SF-TAP on N-terminus were treated as outlined in B. The expression of the receptor was determined in membrane preparations (10 μg) by determining specific binding of a single saturating concentration of [^{3}H]

Molecular Pharmacology Fast Forward. Published on October 29, 2014 as DOI: 10.1124/mol.114.094045
This article has not been copyedited and formatted. The final version may differ from this version.

DPCPX (15 nM). Data are means ± S.E.M from 3 experiments. Statistically significant differences were assessed by repeated-measures ANOVA followed by Tukey's post hoc test (*, $p<0.05$). **D) Accumulation of the mature mutant A_1-receptor-$Y^{288}A$ upon combined inhibition of adenosine kinase, adenosine deaminase and adenosine transport is independent of the translation rate.** HEK293 cells stably expressing A_1-receptor-$Y^{288}A$ fused to YFP were pre-incubated for 4 h with vehicle (lane labeled untreated), 1 μM DPCPX as positive control or 2 μM EHNA, 0.5 μM iodotubercidin and 10 μM dipyridamole (inhibitors c.). Therefater (time = 0), cycloheximide (50 μg/ml) was added to the cells. Cells were then incubated for 2 or 4 hours in the absence or continued presence of the DPCPX or the inhibitor combination. Subsequently, membranes (15 μg/lane) prepared form these cells were electrophoretically resolved and the receptor detected by blotting for the YFP-moiety (upper blot). Immunodetection of G protein β-subunits served as loading control (lower blot).

Figure 3. **Increase in radioligand binding to A_1-adenosine receptor-$Y^{288}A$ in membranes of cells subjected to combined inhibition of adenosine kinase, adenosine deaminase and adenosine transport**. HEK293 cells stably expressing the A_1-receptor-$Y^{288}A$ fused via its C-terminus to YFP (A) or tagged on its N-terminus with SF-TAP (B, C) were incubated for 24 hours with vehicle (white bar), 1 μM DPCPX (light grey) or the combination of inhibitors (dark grey). Receptor levels were determined by incubating membranes (10 μg) prepared from these cells with a single concentration of [^{3}H]DPCPX (A & B; 6 nM) or the indicated concentrations of the radioligand (C). Shown is the specific binding. Non-specific binding was determined in the presence of 10 μM XAC and was below 20% at 6 nM. Data in panels A and B are means ±

Molecular Pharmacology Fast Forward. Published on October 29, 2014 as DOI: 10.1124/mol.114.094045
This article has not been copyedited and formatted. The final version may differ from this version.

S.E.M from 3 and 4 experiments, respectively, and were compared by repeated-measures ANOVA followed by Tukey's post hoc (*, $p<0.05$; **, $p<0.01$ versus control).

Figure 4. **Combined inhibition of adenosine kinase, deaminase and transport does not result in the accumulation of folding-deficient V_2-vasopressin receptor mutants on the cell surface.** HEK293 cells stably expressing N-terminally Flag-tagged V_2-receptor-$I^{318}S$ (A), V_2-receptor-$T^{273}R$-GFP (B) or A_1-receptor-$Y^{288}A$-YFP (C) were incubated with vehicle, the cognate antagonist as a pharmacochaperone (5 μM and 10 μM SR121463A in A and B, respectively; 1 μM DPCPX in C) or the combination of 2 μM EHNA, 0.5 μM 5-iodotubercidin and 10 μM dipyridamole (inhibitors c.). After 24 hours, receptor expression was analyzed by quantifying fluorescence intensity (emitted by YFP/GFP in A &C and by Alexa Fluor® 488-labelled secondary antibody against the primary anti-FLAG antibody, B) by flow cytometry. Shaded histograms represent untreated samples and open histogram indicates the treatment with a pharmacochaperone or the combination of inhibitors. Bar diagrams show means ± S.E.M from three independent experiments performed in triplicates. Statistically significant differences were assessed by repeated-measures ANOVA followed by Tukey's post hoc test (***$p<0.001$).

Figure 5. **Concentration-dependent effect of 5-iodotubercidin, EHNA and dipyridamole on the cellular accumulation of A_1-adenosine receptor-$Y^{288}A$.** A) HEK293 cells stably expressing YFP-tagged A_1-receptor -$Y^{288}A$ were incubated in the absence (control, shaded histogram) or in the presence of the indicated concentrations of each inhibitor, *i.e*. 5-iodotubercidin (IODO), EHNA or dipyridamole (DIP) (open histogram), while the other two inhibitors were kept at a constant concentration of 2 μM, 0.5 μM and 10 μM for EHNA, iodotubercidin and dipyridamole,

Molecular Pharmacology Fast Forward. Published on October 29, 2014 as DOI: 10.1124/mol.114.094045
This article has not been copyedited and formatted. The final version may differ from this version.

respectively. After 24 h, the cells were analyzed by flow cytometry for YFP fluorescence. The histograms are representative of three independent experiments. B) The geometric means of the fluorescence increases shown in panel A were normalized by setting the maximum increase 1 to allow for interassay comparison and plotted to generate concentration-response curves. C) As a control, the cells were incubated in the sole presence of each individual inhibitor, *i.e.* 10 μM dipyridamole (upper histogram), 2 μM EHNA (middle) or 0.5 μM 5-iodotubercidin (bottom) and analyzed as above. Histograms are representative of three independent experiments.

Figure 6. **Concentration-dependent increase in A_1-adenosine receptor-$Y^{288}A$ (A-C) immunoreactivity and antagonist binding (D) after incubation of cells in the presence of 5-iodotubercidin, EHNA and dipyridamole.** HEK293 cells stably expressing YFP-tagged A_1-receptor -$Y^{288}A$ were incubated as outlined in the legend to Fig. 4 in presence of the indicated concentrations of each inhibitor, *i.e.* 5-iodotubercidin (A,D), dipyridamole (B) or EHNA (C), while the other two inhibitors were kept at a constant concentration of 2 μM, 0.5 μM and 10 μM for EHNA, iodotubercidin and dipyridamole, respectively. After 24 h, membranes were prepared and the levels of A_1-receptor were analyzed by immunoblotting for YFP (A-C) with immunoreactivity for Gβ-subunits as a loading control. Alternatively, the receptor was detected by binding of the antagonist radioligand [^{3}H]DPCPX (2.5 nM) (D).

Figure 7. **Hypoxia recapitulates the effect of combined inhibition of adenosine kinase, deaminase and transport and promotes accumulation of A_1-adenosine receptor-$Y^{288}A$.** A) HEK293 cells stably expressing A_1-receptor-$Y^{288}A$-YFP receptor were incubated under normoxic or hypoxic conditions (5% O_2) for 24 h. The A_1-receptor level was detected by immunoblotting

Molecular Pharmacology Fast Forward. Published on October 29, 2014 as DOI: 10.1124/mol.114.094045
This article has not been copyedited and formatted. The final version may differ from this version.

of membrane proteins (20 μg) for the YFP. Gβ-subunits were visualized as a loading control. The blot represents two of three separate experiments. The right-hand bar diagram shows the densitometric quantification of the receptor levels, analyzed by ImageJ software. The relative optical density of mature (M) and core (C) glycosylated species was determined and presented as the M:C ratio. Data are means from three independent experiments, error bars represent S.E.M. The statistical significance of the difference was assessed by a paired t test (*, $p<0.05$). B) HEK293 cells stably expressing A_1-receptor-Y^{288}A-YFP were incubated for 1 or 2 hours with vehicle (white bar), 1 μM DPCPX (light grey), the combination of inhibitors, *i.e*. 2 μM EHNA, 0.5 μM iodotubercidin and 10 μM dipyridamole (dark grey) or subjected to hypoxic conditions (black; 5% O_2). The cell membranes were harvested and receptor levels were determined by immunoblotting for the YFP moiety and by visualizing Gβ-subunits as a loading control. C) Receptor levels were also assessed by measuring specific binding of [^{3}H]DPCPX (6 nM) to membranes of cells that had been subjected to the indicated manipulations for 1 h. Data are means ± S.E.M from 2 separate experiments.

Figure 8. **Increase in wild type A_1-receptor levels in response to combined inhibition of adenosine kinase, deaminase and transport and to hypoxia.** HEK293 cells stably expressing the wild type A_1-receptor with a FLAG-epitope on the N-terminus were incubated for 24 h with vehicle, 1 μM DPCPX or the combination of inhibitors, *i.e.* 2 μM EHNA, 0.5 μM 5-iodotubercidin and 10 μM dipyridamole (inhibitors c.). Subsequently, the expression of the receptor was analyzed by flow cytometry (A, B) or by radioligand saturation binding (C, D). A) Shaded and open histogram represents vehicle-treated control cells and cells exposed to the combination of inhibitors, respectively. B) The fluorescence intensities of three separate

Molecular Pharmacology Fast Forward. Published on October 29, 2014 as DOI: 10.1124/mol.114.094045
This article has not been copyedited and formatted. The final version may differ from this version.

experiments done as illustrated in panel A were quantified as geometric means. Error bars represent S.E.M. C) Membranes were prepared from cells subjected to the conditions outlined above and incubated with the indicated concentrations of the antagonist radioligand [^{3}H]DPCPX. Data are means from duplicate determinations in a representative experiment. The curves represent specific binding. D) B_{max} values are means ± S.E.M from three separate saturation binding experiments. *, $p<0.05$ when compared to the vehicle control by repeated-measures ANOVA followed by Tukey's post hoc test. E) HEK293 cells stably expressing the wild type A_1-receptor tagged with YFP were incubated for 24 h under normoxic or hypoxic conditions (5% O_2) in the absence and presence of the combined inhibitors (inhibitors c.). A_1-receptors were quantified in cell membranes (15 μg of protein) by immunoblotting for the YFP-moiety and for Gβ-subunits as loading control. The blot represents one of three independent experiments. F) HEK293 cells stably expressing wild type A_1-receptor tagged with an SF-TAP epitope on its N-terminus were incubated under normoxic or hypoxic conditions (5% O_2) for 24 h. The expression of the receptor was determined in membrane preparations by saturation binding with the indicated concentrations of [^{3}H]DPCPX. Data are means from duplicate determinations in a representative experiment. G) The experiment depicted in panel G was done on HEK293 cells stably expressing differently N-terminally tagged versions of the wild type A_1-receptor (FLAG or SF-TAP). The expression of the receptor was determined in membrane preparations by determining specific binding of a single saturating concentration of [^{3}H]DPCPX (10 nM). Shown is the fold increase over control (expression level in hypoxia over normoxia) to account for variations in expression levels in the different cell lines. Error bars represent S.E.M (n=8), *, $p< 0.05$, paired t-test.

Fig. 1

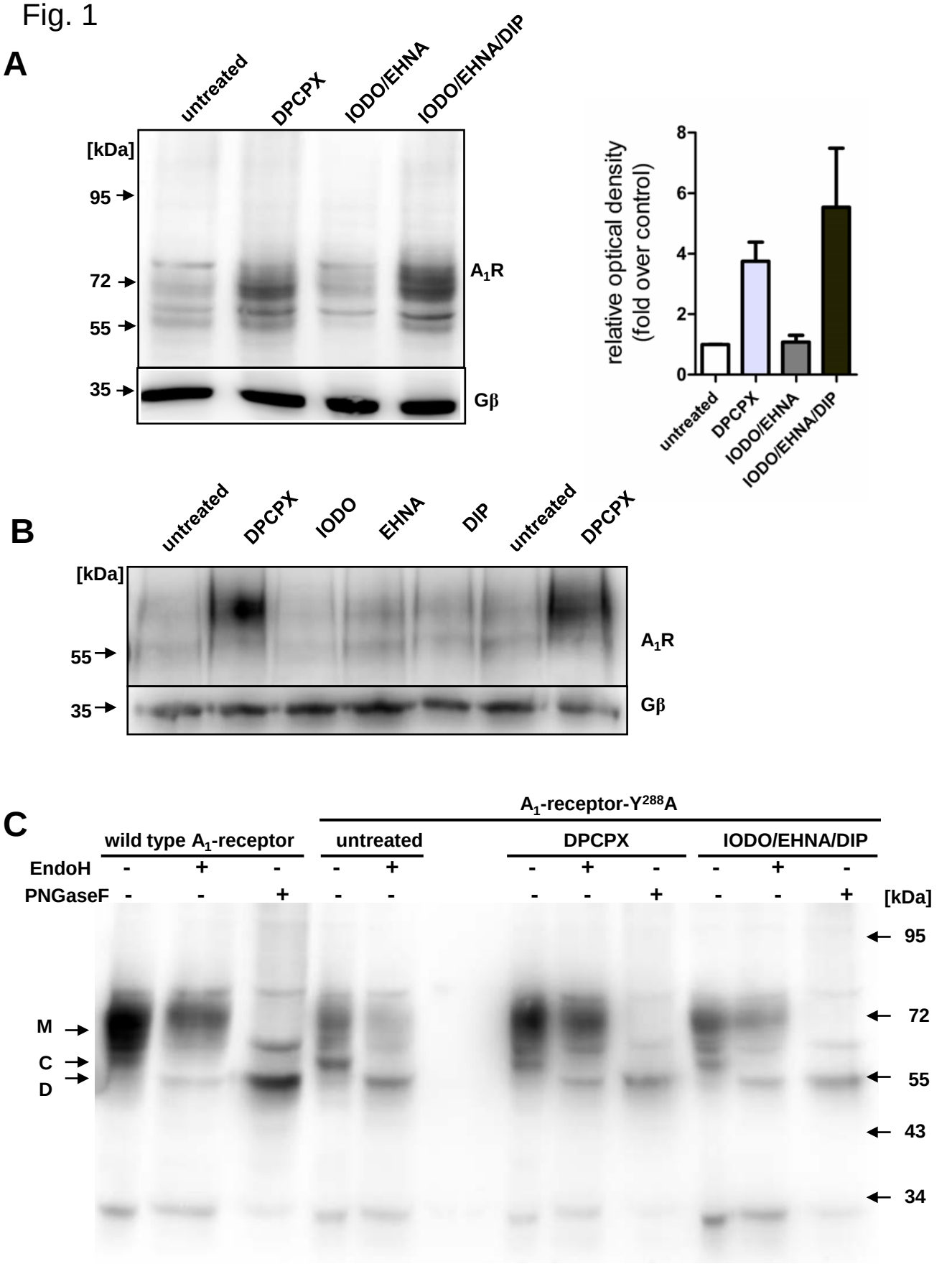
A
untreated
DPCPX
IODO/EHNA
IODO/EHNA/DIP
[kDa]
95
72
55
35
A1R
Gβ
relative optical density
(fold over control)
8
6
4
2
0
untreated
DPCPX
IODO/EHNA
IODO/EHNA/DIP
B
untreated
DPCPX
IODO
EHNA
DIP
untreated
DPCPX
[kDa]
55
35
A1R
Gβ
C
A1-receptor-Y288A
wild type A1-receptor
untreated
DPCPX
IODO/EHNA/DIP
EndoH
PNGaseF
[kDa]
95
72
55
43
34
M
C
D

Fig. 2

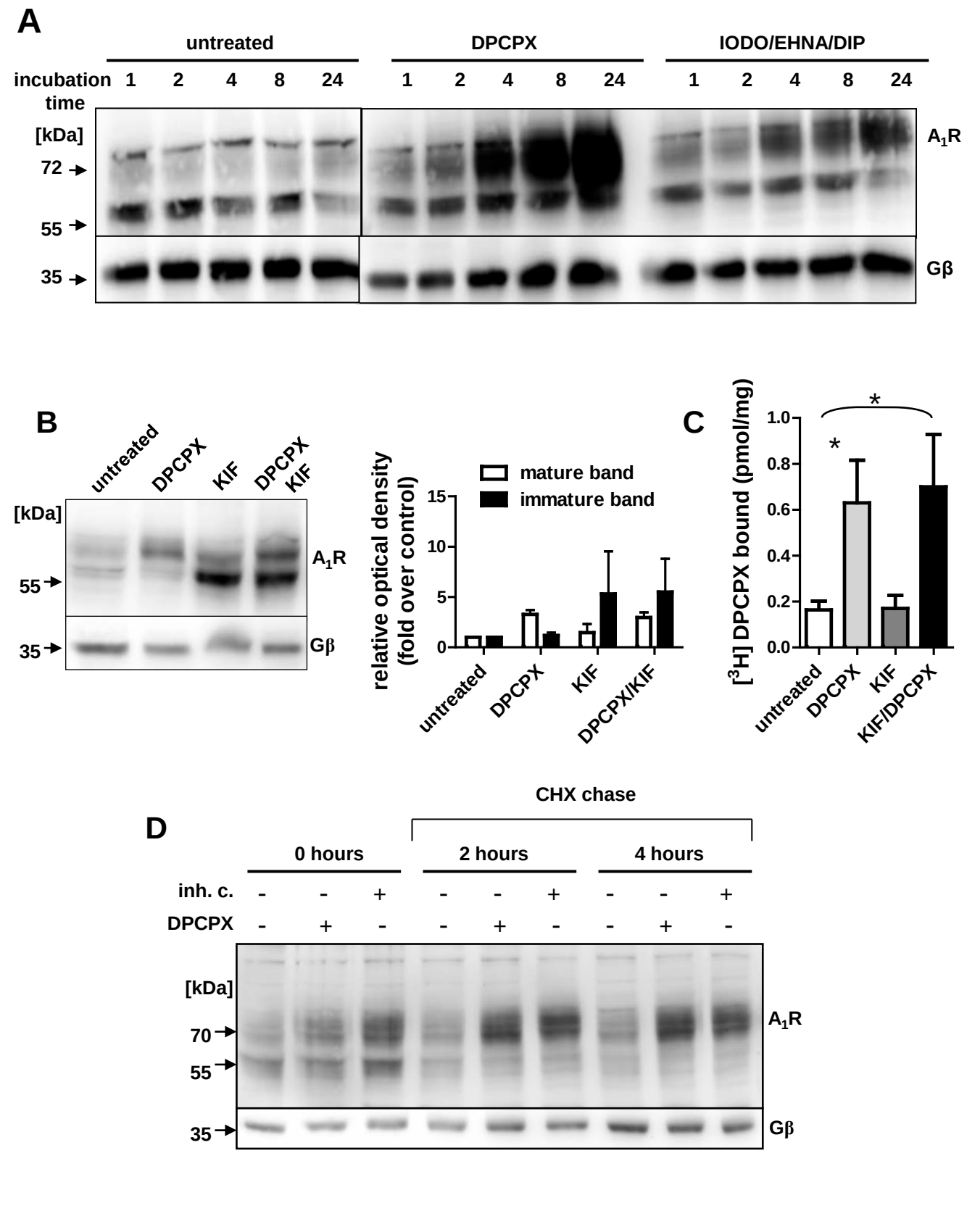
A
untreated
DPCPX
IODO/EHNA/DIP
incubation time
1 2 4 8 24
[kDa]
72
55
35
A1R
Gβ
B
untreated
DPCPX
KIF
DPCPX KIF
[kDa]
55
35
A1R
Gβ
relative optical density (fold over control)
mature band
immature band
untreated
DPCPX
KIF
DPCPX/KIF
C
[3H] DPCPX bound (pmol/mg)
untreated
DPCPX
KIF
KIF/DPCPX
D
CHX chase
0 hours
2 hours
4 hours
inh. c.
DPCPX
[kDa]
70
55
35
A1R
Gβ

Fig. 3

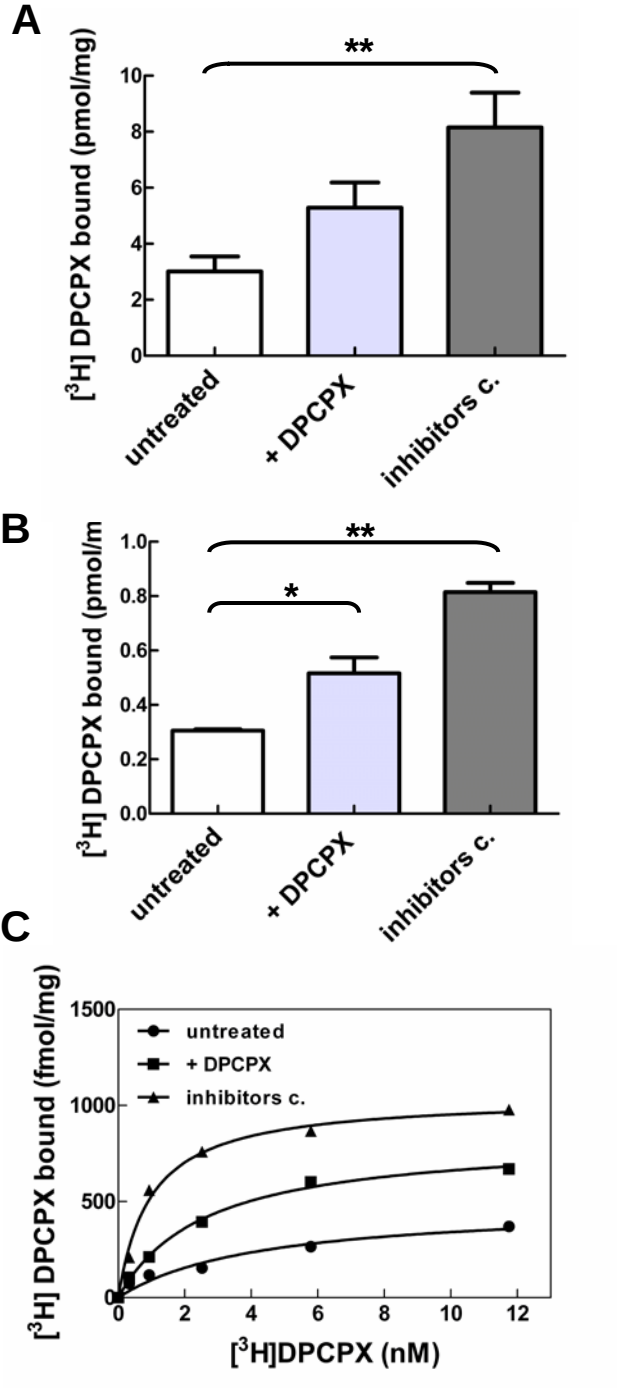
A
**
[3H] DPCPX bound (pmol/mg)
10
8
6
4
2
0
untreated
+ DPCPX
inhibitors c.
B
**
*
[3H] DPCPX bound (pmol/m
1.0
0.8
0.6
0.4
0.2
0.0
untreated
+ DPCPX
inhibitors c.
C
[3H] DPCPX bound (fmol/mg)
1500
1000
500
0
untreated
+ DPCPX
inhibitors c.
0
2
4
6
8
10
12
[3H]DPCPX (nM)

Fig. 4

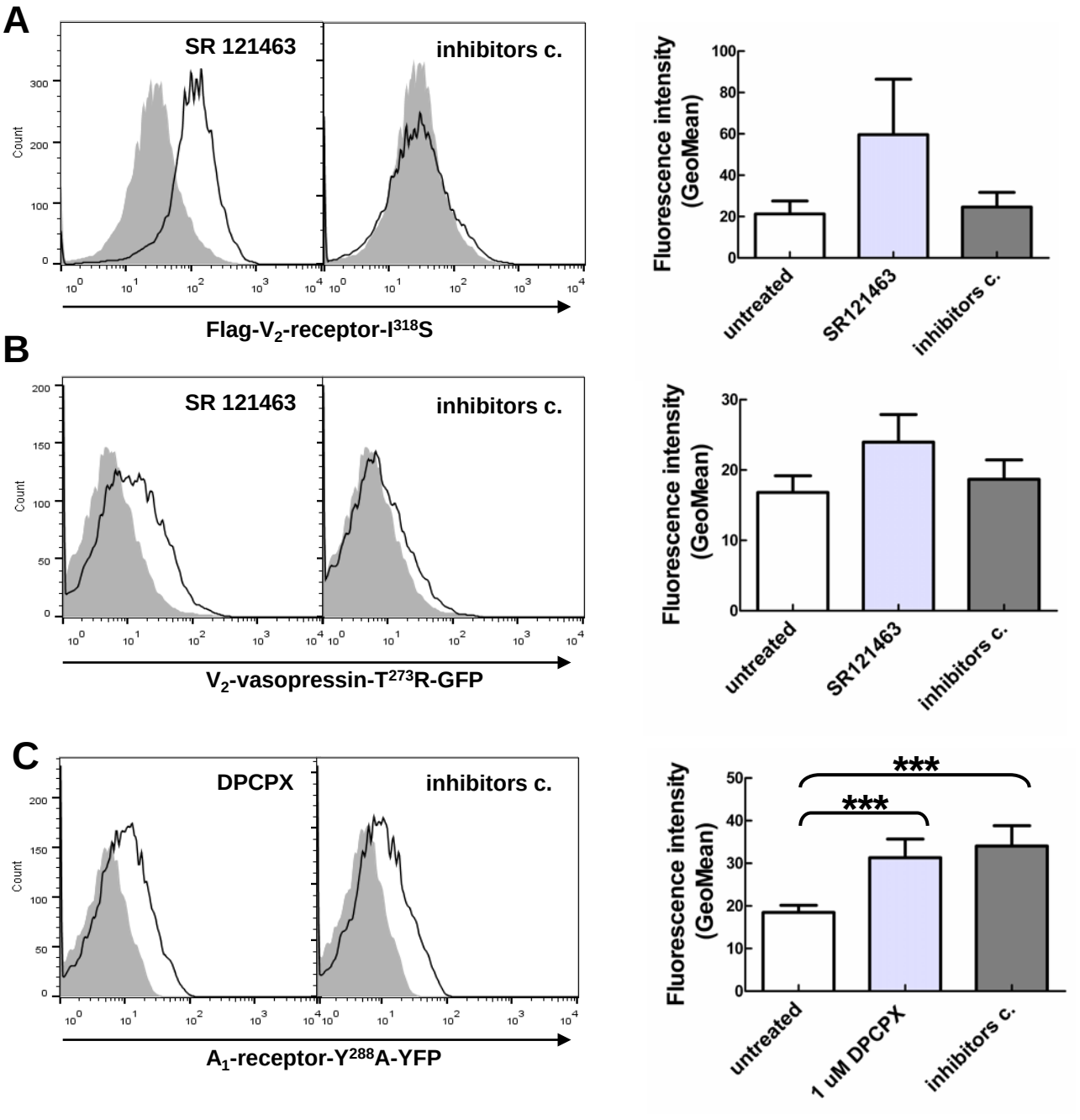
A
SR 121463
inhibitors c.
Count
Flag-V2-receptor-I318S
Fluorescence intensity (GeoMean)
untreated
SR121463
inhibitors c.
B
SR 121463
inhibitors c.
Count
V2-vasopressin-T273R-GFP
Fluorescence intensity (GeoMean)
untreated
SR121463
inhibitors c.
C
DPCPX
inhibitors c.
Count
A1-receptor-Y288A-YFP
Fluorescence intensity (GeoMean)
***
***
untreated
1 uM DPCPX
inhibitors c.

Fig. 5

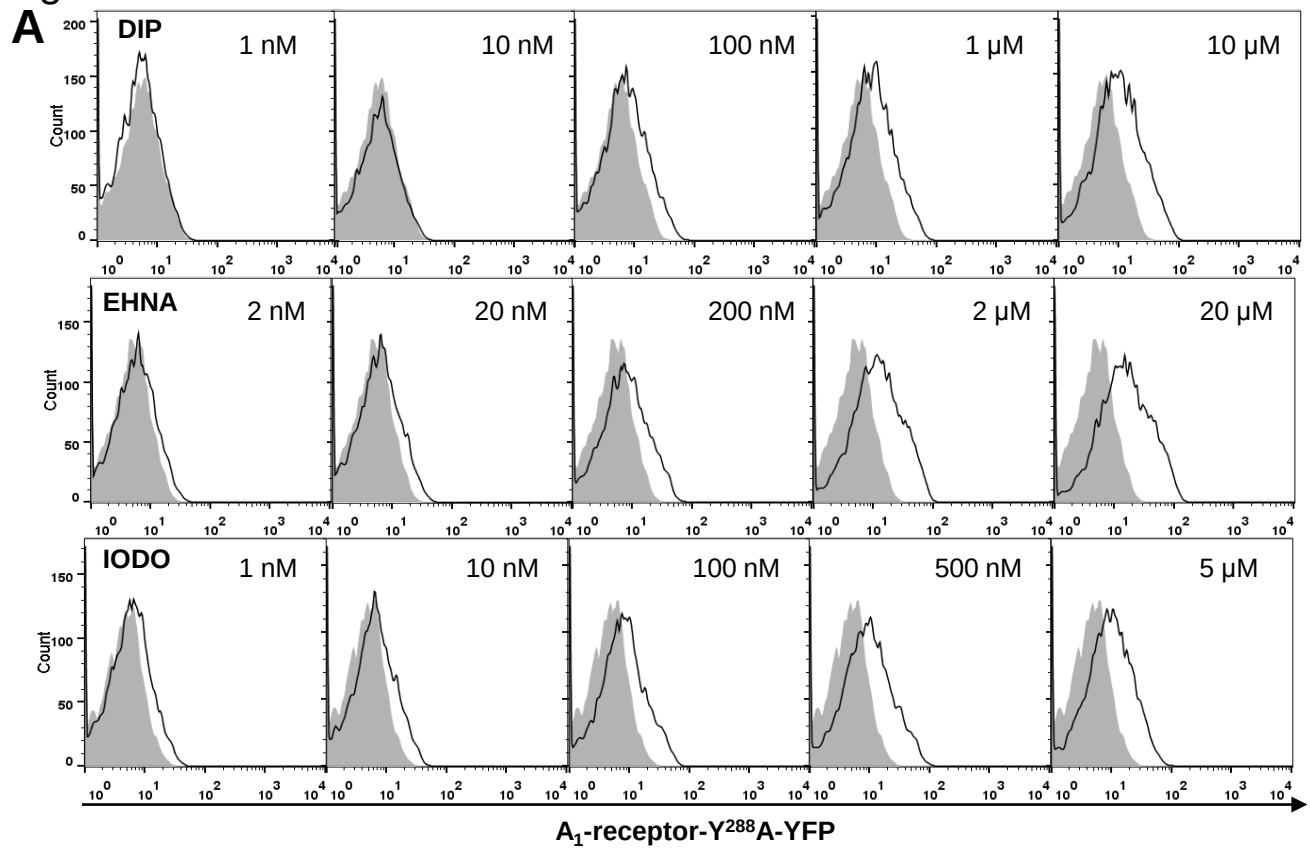
A
DIP
1 nM
10 nM
100 nM
1 µM
10 µM
EHNA
2 nM
20 nM
200 nM
2 µM
20 µM
IODO
1 nM
10 nM
100 nM
500 nM
5 µM
Count
A1-receptor-Y288A-YFP

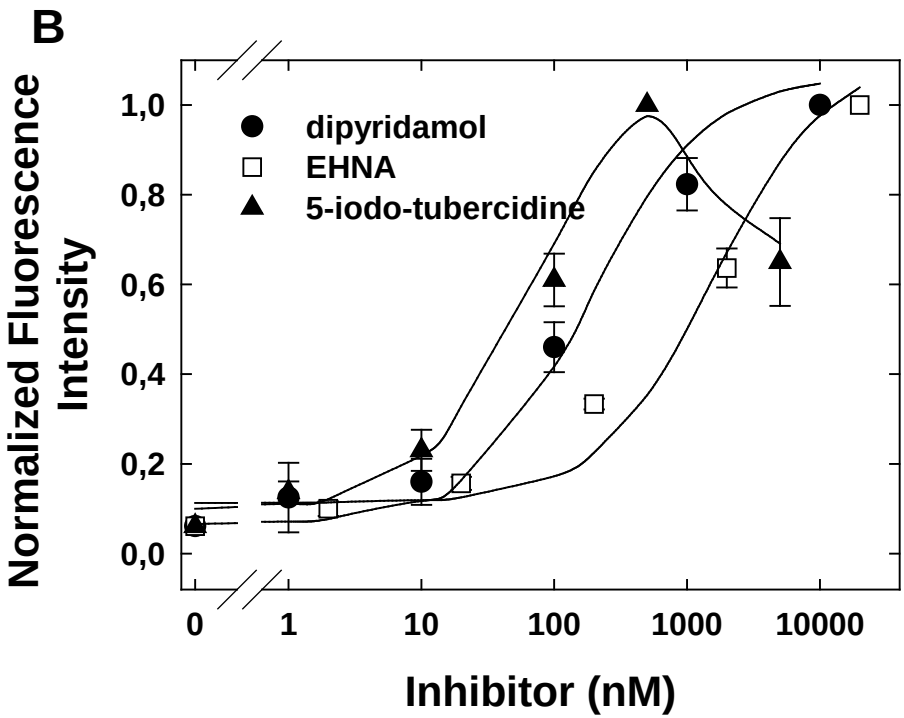
B
Normalized Fluorescence Intensity
dipyridamol
EHNA
5-iodo-tubercidine
Inhibitor (nM)

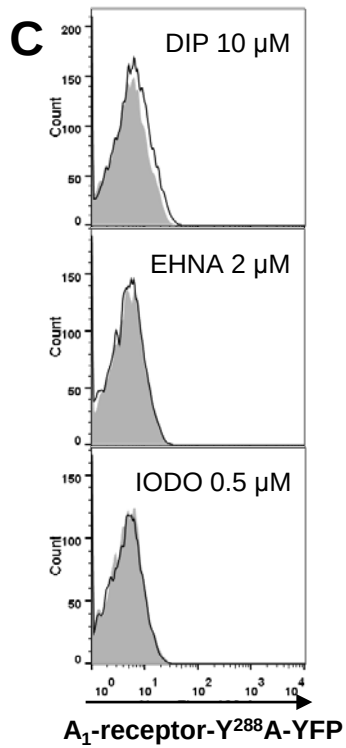
C
DIP 10 µM
EHNA 2 µM
IODO 0.5 µM
Count
A1-receptor-Y288A-YFP

Fig. 6

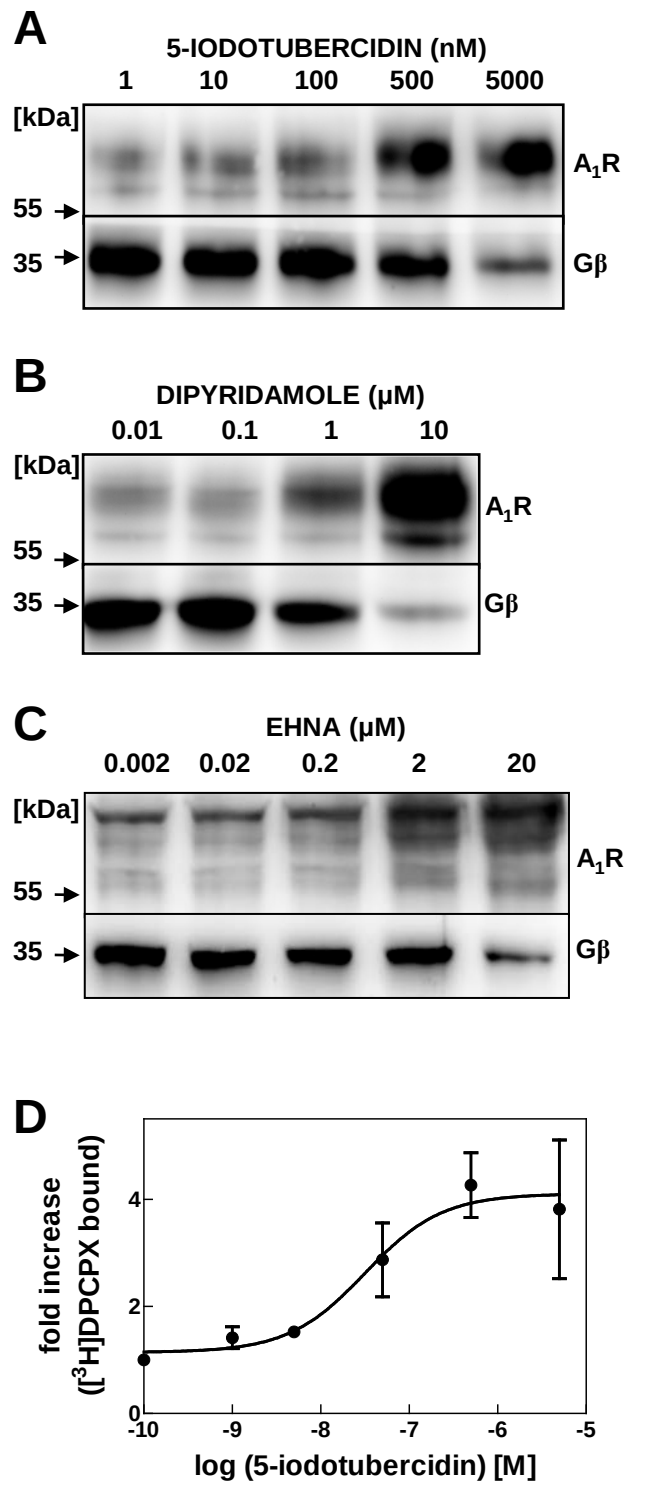
A
5-IODOTUBERCIDIN (nM)
1
10
100
500
5000
[kDa]
55
35
A1R
Gβ
B
DIPYRIDAMOLE (μM)
0.01
0.1
1
10
[kDa]
55
35
A1R
Gβ
C
EHNA (μM)
0.002
0.02
0.2
2
20
[kDa]
55
35
A1R
Gβ
D
fold increase
([3H]DPCPX bound)
0
2
4
-10
-9
-8
-7
-6
-5
log (5-iodotubercidin) [M]

Fig. 7

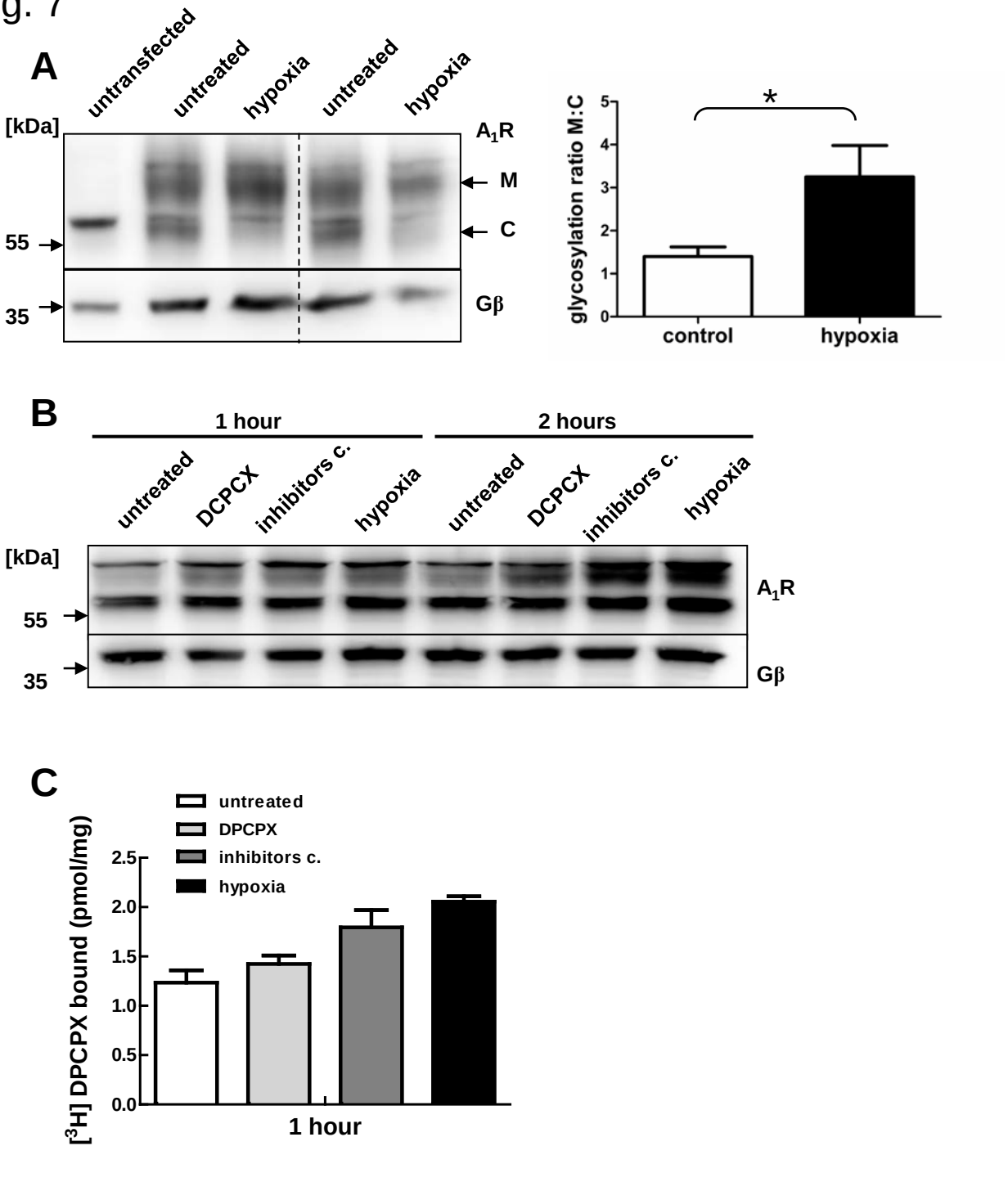
A
untransfected
untreated
hypoxia
untreated
hypoxia
[kDa]
55
35
A1R
M
C
Gβ
glycosylation ratio M:C
*
control
hypoxia
B
1 hour
2 hours
untreated
DCPCX
inhibitors c.
hypoxia
untreated
DCPCX
inhibitors c.
hypoxia
[kDa]
55
35
A1R
Gβ
C
untreated
DPCPX
inhibitors c.
hypoxia
[3H] DPCPX bound (pmol/mg)
1 hour

Fig. 8

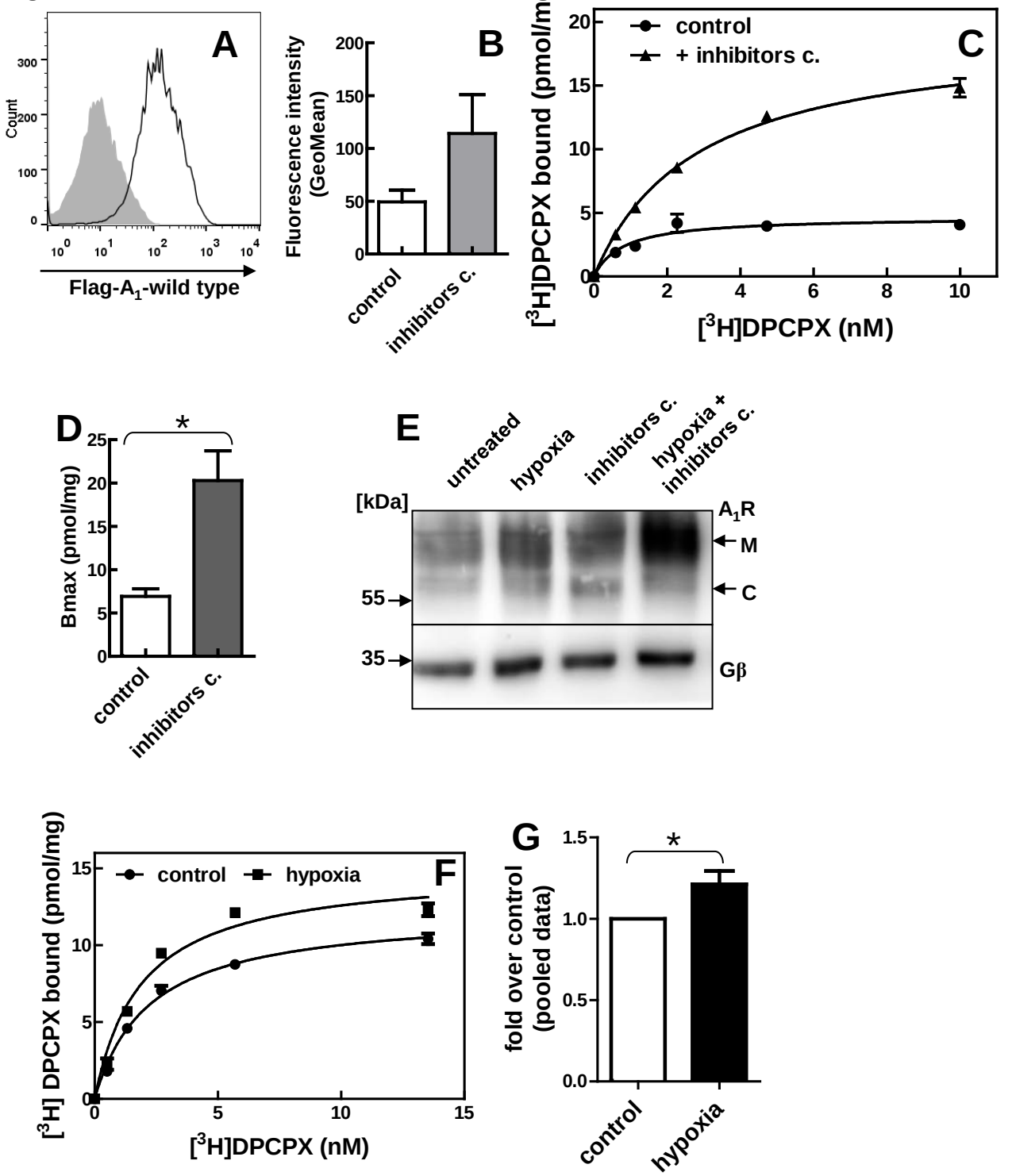
A
Count
Flag-A1-wild type
B
Fluorescence intensity (GeoMean)
control
inhibitors c.
C
control
+ inhibitors c.
[3H]DPCPX bound (pmol/mg)
[3H]DPCPX (nM)
D
Bmax (pmol/mg)
control
inhibitors c.
E
untreated
hypoxia
inhibitors c.
hypoxia + inhibitors c.
[kDa]
A1R
M
C
55
35
Gβ
F
control
hypoxia
[3H] DPCPX bound (pmol/mg)
[3H]DPCPX (nM)
G
fold over control (pooled data)
control
hypoxia